HHS Public Access

Author manuscript

Nanoscale. Author manuscript; available in PMC 2016 May 30.

Published in final edited form as:

Nanoscale. 2015 June 21; 7(23): 10330–10333. doi:10.1039/c5nr01833a.

Folic acid conjugated ferritins as photosensitizer carriers for photodynamic therapy†

Zipeng Zhen[a,b], **Wei Tang**[a,b], **Weizhong Zhang**[a,b], and **Jin Xie**[a,b]

Jin Xie: jinxie@uga.edu

[a]Department of Chemistry, University of Georgia, Athens, Georgia 30602, United States

[b]Bio-Imaging Research Center, University of Georgia, Athens, Georgia 30602, United States

Abstract

We coupled folic acid as a tumour targeting ligand to the surface of ferritins and loaded them with $ZnF_{16}Pc$. The resulting nanoconjugates can efficiently home to 4T1 tumours *in vivo*, and, with photoirradiation, leading to suppressed tumour growth and tumour metastasis.

Photodynamic therapy (PDT) is a relatively new treatment modality that has shown great promise in cancer management.[1–3] In a typical PDT session, photosensitizers are first injected to patients, followed by photoirradiation to the diseased areas (e.g. tumours) at appropriate drug-light intervals.[4,5] Given that photosensitizers are often low-toxic in the dark, the treatment can be confined to the areas of irradiation, causing little systematic toxicity. In reality, however, PDT is often associated with side effects, particularly to the skin and eyes.[6,7] This is because conventional photosensitizers have poor tumour-to-normal tissue selectivity.[8,9] Even for newer generation photosensitizers, the administered patients have to stay away from sun light or even room light to avoid phototoxicity.[10] To address the issue, there have been continuous efforts on developing a photosensitizer nanocarrier, be it polymer-,[11] metal-,[12] or silica[13]-based, that can deliver photosensitizers to tumours in a site-specific fashion. Very recently, our group reported that ferritin, a natural protein nanocage, can load $ZnF_{16}Pc$, a near-infrared (NIR) photosensitizer, at extremely high efficiency (up to 60 wt%).[14] When surface-modified with RGD4C, ferritins can efficiently deliver $ZnF_{16}Pc$ to tumours, while minimally accumulating in the skin.[14]

PDT can either target cancer cells or tumour vasculatures.[15,16] For vascular targeting PDT, the photodynamic damage is mostly inflicted on neoplastic vasculatures, which leads to formation of thrombi and destruction of blood vessels, and in turn, tissue ischemia.[2,17] For instance, our previous exploits with RGD4C-modified ferritins are making use of the vasculature-targeting mechanism.[18,19] In the present study, we assess the feasibility of engineering ferritins for cancer cell targeting PDT. To this end, we coupled folic acid as a tumour targeting ligand to the surface of ferritins. The target, folic acid receptor, is found to be overexpressed in about 40% human cancers, and is able to mediate endocytosis of folic

†Electronic Supplementary Information (ESI) available: Details of experiments and *ex vivo* imaging results. See DOI: 10.1039/c000000x/

Correspondence to: Jin Xie, jinxie@uga.edu.

acid conjugated cargos.[20–22] Specifically, we prepared $ZnF_{16}Pc$ (a potent photosensitizer) loaded and folic acid conjugated ferritins (hereafter referred to as P@FA-FRTs) and injected them into 4T1 tumour bearing BLAB/c mice. P@FA-FRTs were found to be able to efficiently home to and retain in 4T1 tumours, which is attributed to folic acid receptor-mediated internalization. With photoirradiation, the treatment caused efficient tumour growth inhibition, while not inducing detectable side effects to the host. Interestingly, the PDT also led to suppressed cancer metastasis to the lung, suggesting the involvement of a PDT stimulated anti-tumour immune response to the treatment.

We used human heavy chain ferritins throughout the whole study. The expression, production, and purification of ferritins were reported by us before.[18] In previous studies, we have successfully conjugated dyes[23] and peptides[24] to the surface of ferritins. Similar conjugation chemistry was used to achieve coupling of folic acid to ferritins.[25] The folic acid coupled ferritins can still efficiently load $ZnF_{16}Pc$, yielding P@FA-FRTs.[26]Although it is possible to achieve formulations of even higher $ZnF_{16}Pc$ loading rates,[14] we used a 40wt % formulation for the present study. This is based on the consideration that further increasing the loading rate may lead to compromised particle colloidal stability and/or cause self-quenching. The same loading rate was used for studies with RGD modified ferritins in our previous studies.[14]

Targeting specificity and internalization was investigated *in vitro* with 4T1 cells, which is folic acid receptor positive.[27,28] To facilitate the tracking of ferritins, P@FA-FRTs were labelled with IRDye800 (ex/em: 780/800 nm). For comparison, $ZnF_{16}Pc$ loaded parental ferritins were also investigated. Compared to ferritins, P@FA-FRTs display much higher uptake by 4T1 cells (Fig. 1a). Fluorescence microscopy found strong fluorescence signals evenly distributed in the cell plasma (Fig. 1a). The uptake was attributed to folic acid receptor mediated endocytosis, which was observed previously with other types of nanoparticles that were coupled with folic acid.[29–31]

Next, we investigated cell toxicity by both 3-(4,5-dimethylthiazol-2-yl)-2,5-diphenyltetrazolium bromide (MTT) assay and ethidium homodimer-1 assay (EthD-1,a.k.a. dead assay). In the dark, P@FA-FRTs induced little toxicity to cells; but when the incubation was followed by 671-nm irradiation (100 mW/cm^2, 200 seconds), extensive cell death was observed (Fig. 1b). The toxicity is dependent on the incubation time and P@FA-FRT concentration. When the incubation time was fixed at 24 h, the cell survival was inversely correlated to the drug dose, showing viability values of 89.85 ± 9.22, 82.37 ± 1.66, 62.83 ± 2.90, 45.84 ± 3.55, and 20.91 ± 7.96% at a $ZnF_{16}Pc$ concentration of 3, 6.25, 12.5, 25, and 50 μg/mL, respectively (Fig. 1b). Meanwhile, when the $ZnF_{16}Pc$ concentration was maintained (50 μg/mL), there was clearly an increased level of cell death when the incubation time was extended (Fig. 1c).

The *in vivo* studies were performed in 4T1 tumour bearing BALB/c mice. This is different from our previous investigations, where immunodeficient mice were used for tumour model establishment.[14] One concern with the change, however, is that our ferritins are human origin. Hence, the injected ferritin formulations are potentially immunogenic and may cause immune response that is detrimental or even lethal to the host. Hence, before therapy studies,

we conducted a safety study with normal BALB/c mice. Specifically, we injected large doses of ferritins, either intraperitoneally (i.p., 50 mg/kg) or intravenously (i.v., 15 mg/kg), to normal BALB/c mice and observed the animals for 2 weeks (Fig. 2). Except for a seemingly minor weight loss in the first 24 h, there was no significant weight change in the observation period (Fig. 2). In addition, there was no sign of severe acute inflammation or other abnormalities, suggesting good tolerance of the host to ferritins. This is not unexpected because the human and mouse ferritins share a great deal of similarity. In particular, there is a 93% similarity in amino acids sequence between human and mouse heavy chain ferritins.[32]

Next, we set out to study the targeting specificity of P@FA-FRTs in 4T1 tumour bearing animals. Specifically, IRDye800 labelled P@FA-FRTs were i.v. injected (5 mg/kg); fluorescence images were acquired at different time points on a Maestro II imaging system using a NIR filter (750 to 940 nm). The tumour areas were shaven to minimize interference by hairs. For control, $ZnF_{16}Pc$-loaded FRTs (P@FRTs, 40wt% loading rate, IRDye800 labelled) were administered and evaluated. For P@FRTs, the nanoparticles were concentrated in the tumours at early time points (Fig. 3a), but were gradually cleared from the area. At 24 h, only weak signals were retained in tumours (Fig. 3a). For P@FA-FRTs, on the other hand, there was a much higher level of fluorescence signal retained in tumours at 4 h or even 24 h. The difference in tumour retention was attributed to the difference in tumour uptake mechanism. For P@FRTs, the tumour accumulation was mainly mediated by the enhanced permeability and retention (EPR) effect. Without specific binding, however, the particles over time may re-enter the circulation or be cleared away by the lymphatic system. For P@FA-FRTs, on the other hand, many of the particles are tethered to cancer cell surface or even internalized by interaction with folic acid receptor, resulting in longer tumour retention. According to the region of interest (ROI) analysis, the tumour uptake of P@FA-FRTs at 24 h was 8.31 ± 1.54 times higher than that of P@FRTs (Fig. 3b Notably, fluorescence activities may slowly drop after particle endocytosis due to dye degradation in the acidic endosome/lysosome environments. Hence, actual difference in tumour uptake of the particles may be even more significant. The difference in tumour uptake was also confirmed by post mortal histology studies (Fig. 3c). Relative to P@FRTs, a high tumour uptake was observed with P@FR-FRTs. Most signals were found outside of the tumour vasculatures (stained by anti-CD31 antibody, labelled with phycoerythrin) and were distributed randomly, suggesting the contribution of EPR effect to the tumour uptake.

We also investigated tumour treatment efficacy with P@FA-FRTs. The same 4T1 tumour models were used for the studies. Specifically, we i.v. injected P@FA-FRTs (1.5 mg $ZnF_{16}Pc$/kg, 40wt%) to the mice and irradiated the tumours at 24 h with a 671-nm laser over a 1-cm diameter beam (300 mW/cm^2, 15 minutes, n = 5). The control animals received PBS only, or P@FA-FRTs without photoirradiation. The tumour growth was monitored over a span of 2 weeks. While P@FA-FRTs alone induced no impact to tumour growth, P@FA-FRTs plus photoirradiation led to significant tumour growth suppression (Fig. 4a&b). Relative to the control animals, the tumour growth inhibition (TGI) rate of the treatment group was 82.65% on day 14 (Fig. 4a). Meanwhile, the treatment did not adversely affect body weight of the animals (Fig. 4c). In fact, there was even a slight increase of body weight for the treatment group on day 14.

To further assess the PDT treatment, we performed H&E staining on tumour and normal tissue samples. These include the lung, which is a common metastasis site for breast cancer. In particular, previous studies with 4T1 rodent models frequently find metastasis to the lung.[33] Indeed, in the two control groups, we observed multiple metastasis sites in the lung, manifesting pathological changes such as thickened alveolar membranes, bleeding, and inflammation (Fig. 4d). In the treatment group, on the other hand, there was no sign of metastasis in the lung as well as other normal tissues. The exact reason behind the suppressed metastasis is unknown. It is postulated, however, that an anti-tumour immune response stimulated by PDT may have contributed. Unlike chemotherapy and radiotherapy, PDT is an immunostimulatory treatment modality. Previous studies have observed that in addition to cellular and vascular effects, PDT induced immune response can also benefit tumour management.[34, 35] More detailed investigation into the anti-tumour immune response will be performed in future studies.

Conclusions

Overall, we have shown that folic acid can be coupled to ferritins that are loaded with photosensitizers like $ZnF_{16}Pc$. The resulting nanoconjugates after systematic injection can efficiently home to tumours. With photoirradiation, the treatment caused efficient tumour growth suppression while minimally affecting normal tissues. More interestingly, it was observed that PDT treatment helped suppress tumour metastasis to the lung, which is likely attributed to a PDT-stimulated anti-tumour response. These observations confirm ferritin as a safe and powerful nanoplatform for efficient delivery of photosensitizers.

Supplementary Material

Refer to Web version on PubMed Central for supplementary material.

Acknowledgement

This research was supported by an NCI/NIH R00 grant (R00CA153772, J.X.), a UGA-GRU seed grant (J.X.), and an Elsa U. Pardee Foundation Award (J.X.).

Notes and references

1. Nkepang G, Bio M, Rajaputra P, Awuah SG, You Y. Bioconjugate Chem. 2014; 25:2175–2188.
2. Dolmans DE, Fukumura D, Jain RK. Nat. Rev. Cancer. 2003; 3:380–387. [PubMed: 12724736]
3. Wang C, Tao H, Cheng L, Liu Z. Biomaterials. 2011; 32:6145–6154. [PubMed: 21616529]
4. Foster TH, Giesselman BR, Hu R, Kenney ME, Mitra S. Transl. Oncol. 2010; 3:135–141. [PubMed: 20360938]
5. Wang J, Xu JA, Chen JY, He Q, Xiang L, Huang XM, Ding GR, Xu SM. Arch. Gynecol. Obstet. 2010; 282:307–312. [PubMed: 20024569]
6. Corti MA, Mainetti C. Photomed. Laser Surg. 2010; 28:697–702. [PubMed: 20961234]
7. Taub AF, Garretson CB. J. Drugs Dermatol. 2011; 10:1049–1056. [PubMed: 22052276]
8. Triesscheijn M, Baas P, Schellens JH, Stewart FA. Oncologist. 2006; 11:1034–1044. [PubMed: 17030646]
9. Vrouenraets MB, Visser GW, Snow GB, van Dongen GA. Anticancer Res. 2003; 23:505–522. [PubMed: 12680139]

10. Allison RR, Downie GH, Cuenca R, Hu XH, Childs CJH, Sibata CH. Photodiagn Photodyn. 2004; 1:27–42.
11. Wang SY, Fan WZ, Kim G, Hah HJ, Lee YEK, Kopelman R, Ethirajan M, Gupta A, Goswami LN, Pera P, Morgan J, Pandey RK. Laser Surg. Med. 2011; 43:686–695.
12. Yoo JJ, Kim C, Chung CW, Jeong YI, Kang DH. Int. J. Nanomed. 2012; 7:1997–2005.
13. Huang P, Lin J, Wang S, Zhou Z, Li Z, Wang Z, Zhang C, Yue X, Niu G, Yang M, Cui D, Chen X. Biomaterials. 2013; 34:4643–4654. [PubMed: 23523428]
14. Zhen Z, Tang W, Guo C, Chen H, Lin X, Liu G, Fei B, Chen X, Xu B, Xie J. ACS Nano. 2013; 7:6988–6996. [PubMed: 23829542]
15. Busch TM, Wang HW, Wileyto EP, Yu G, Bunte RM. Radiat. Res. 2010; 174:331–340. [PubMed: 20726728]
16. Firczuk M, Gabrysiak M, Barankiewicz J, Domagala A, Nowis D, Kujawa M, Jankowska-Steifer E, Wachowska M, Glodkowska-Mrowka E, Korsak B, Winiarska M, Golab J. Cell death Dis. 2013; 4:e741. [PubMed: 23887632]
17. Dolmans DE, Kadambi A, Hill JS, Waters CA, Robinson BC, Walker JP, Fukumura D, Jain RK. Cancer Res. 2002; 62:2151–2156. [PubMed: 11929837]
18. Zhen Z, Tang W, Chen H, Lin X, Todd T, Wang G, Cowger T, Chen X, Xie J. ACS Nano. 2013; 7:4830–4837. [PubMed: 23718215]
19. Zhen Z, Tang W, Chuang YJ, Todd T, Zhang W, Lin X, Niu G, Liu G, Wang L, Pan Z, Chen X, Xie J. ACS Nano. 2014; 8:6004–6013. [PubMed: 24806291]
20. Parker N, Turk MJ, Westrick E, Lewis JD, Low PS, Leamon CP. Anal. Biochem. 2005; 338:284–293. [PubMed: 15745749]
21. Gabizon A, Shmeeda H, Horowitz AT, Zalipsky S. Adv. Drug Delivery Rev. 2004; 56:1177–1192.
22. Low PS, Kularatne SA. Curr. Opin. Chem. Biol. 2009; 13:256–262. [PubMed: 19419901]
23. Lin X, Xie J, Niu G, Zhang F, Gao H, Yang M, Quan Q, Aronova MA, Zhang G, Lee S, Leapman R, Chen X. Nano Lett. 2011; 11:814–819. [PubMed: 21210706]
24. Lin X, Xie J, Zhu L, Lee S, Niu G, Ma Y, Kim K, Chen XY. Angew. Chem. Int. Edit. 2011; 50:1569–1572.
25. Ren Y, Wong SM, Lim LY. Bioconjugate Chem. 2007; 18:836–843.
26. Garcia AM, Alarcon E, Munoz M, Scaiano JC, Edwards AM, Lissi E. Photoch. Photobio. Sci. 2011; 10:507–514.
27. Gao ZG, Tian L, Hu J, Park IS, Bae YH. J. Control. Release. 2011; 152:84–89. [PubMed: 21295088]
28. Reddy JA, Xu LC, Parker N, Vetzel M, Leamon CP. J. Nucl. Med. 2004; 45:857–866. [PubMed: 15136637]
29. Luo Z, Ding X, Hu Y, Wu S, Xiang Y, Zeng Y, Zhang B, Yan H, Zhang H, Zhu L, Liu J, Li J, Cai K, Zhao Y. ACS Nano. 2013; 7:10271–10284. [PubMed: 24127723]
30. Stella B, Arpicco S, Peracchia MT, Desmaele D, Hoebeke J, Renoir M, D'Angelo J, Cattel L, Couvreur P. J. Pharm. Sci. 2000; 89:1452–1464. [PubMed: 11015690]
31. Chen HY, Li SL, Li BW, Ren XY, Li SN, Mahounga DM, Cui SS, Gu YQ, Achilefu S. Nanoscale. 2012; 4:6050–6064. [PubMed: 22930451]
32. Torti SV, Kwak EL, Miller SC, Miller LL, Ringold GM, Myambo KB, Young AP, Torti FM. J. Biol. Chem. 1988; 263:12638–12644. [PubMed: 3410854]
33. Li Y, Jin M, Shao S, Huang W, Yang F, Chen W, Zhang S, Xia G, Gao Z. BMC Cancer. 2014; 14:329. [PubMed: 24885518]
34. de Vree WJ, Essers MC, Koster JF, Sluiter W. Cancer Res. 1997; 57:2555–2558. [PubMed: 9205052]
35. Blank M, Lavie G, Mandel M, Keisari Y. Oncol. Res. 2000; 12:409–418. [PubMed: 11697819]

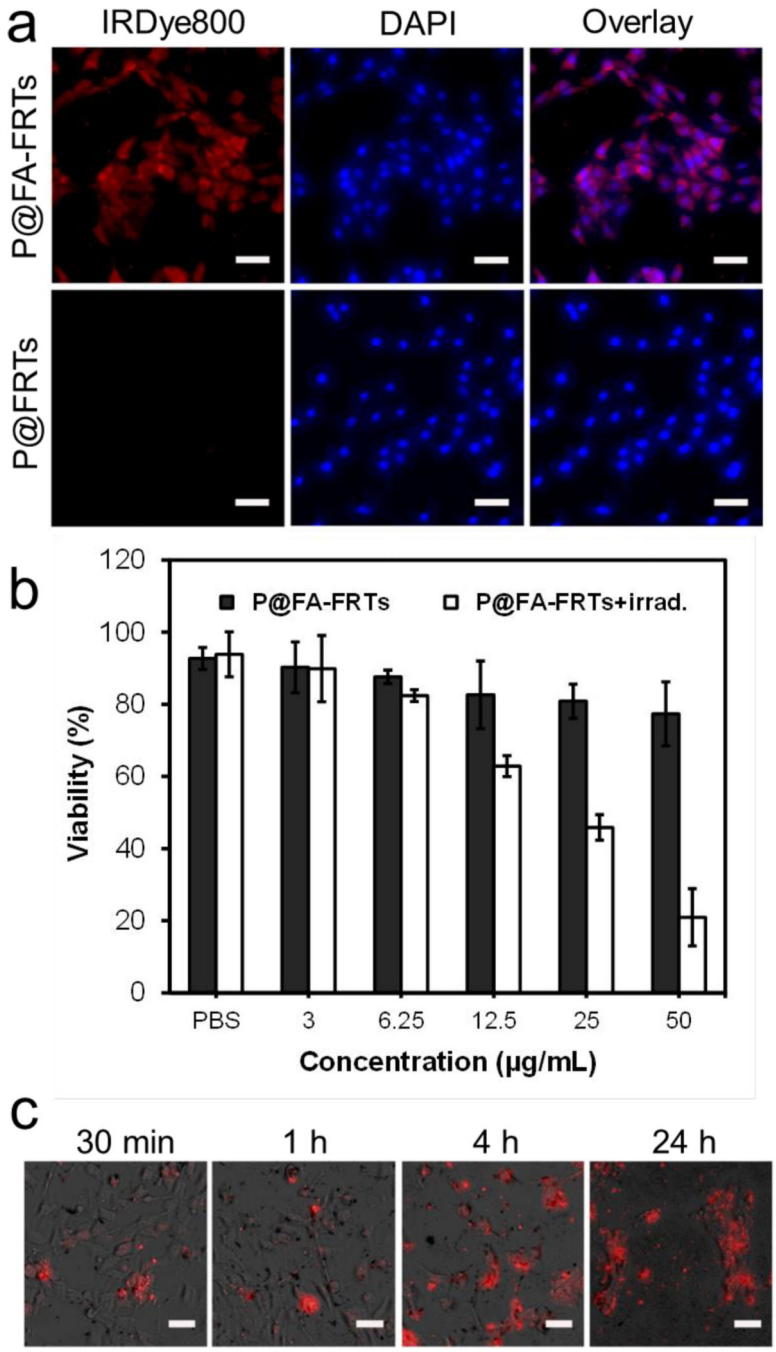

Fig. 1.

(a) Cell uptake studies. P@FA-FRTs (IRDye800 labeled) were efficiently internalized by 4T1 cells while parental ferritins were not. Red, IRDye800; blue, DAPI. Scale bars, 50 μm. (b) MTT cell viability assay results. Concentration dependent cell death was observed with P@FA-FRT-mediated PDT. Light irradiation: 671 nm, 100 mW/cm^2 for 200 s. (c) EthD-1 cell assay results. When extending the incubation time, there was an increased level of cell death, marked as red fluorescence. Red, EthD-1 (ex/em = 528/617 nm). Scale bars, 50 μm.

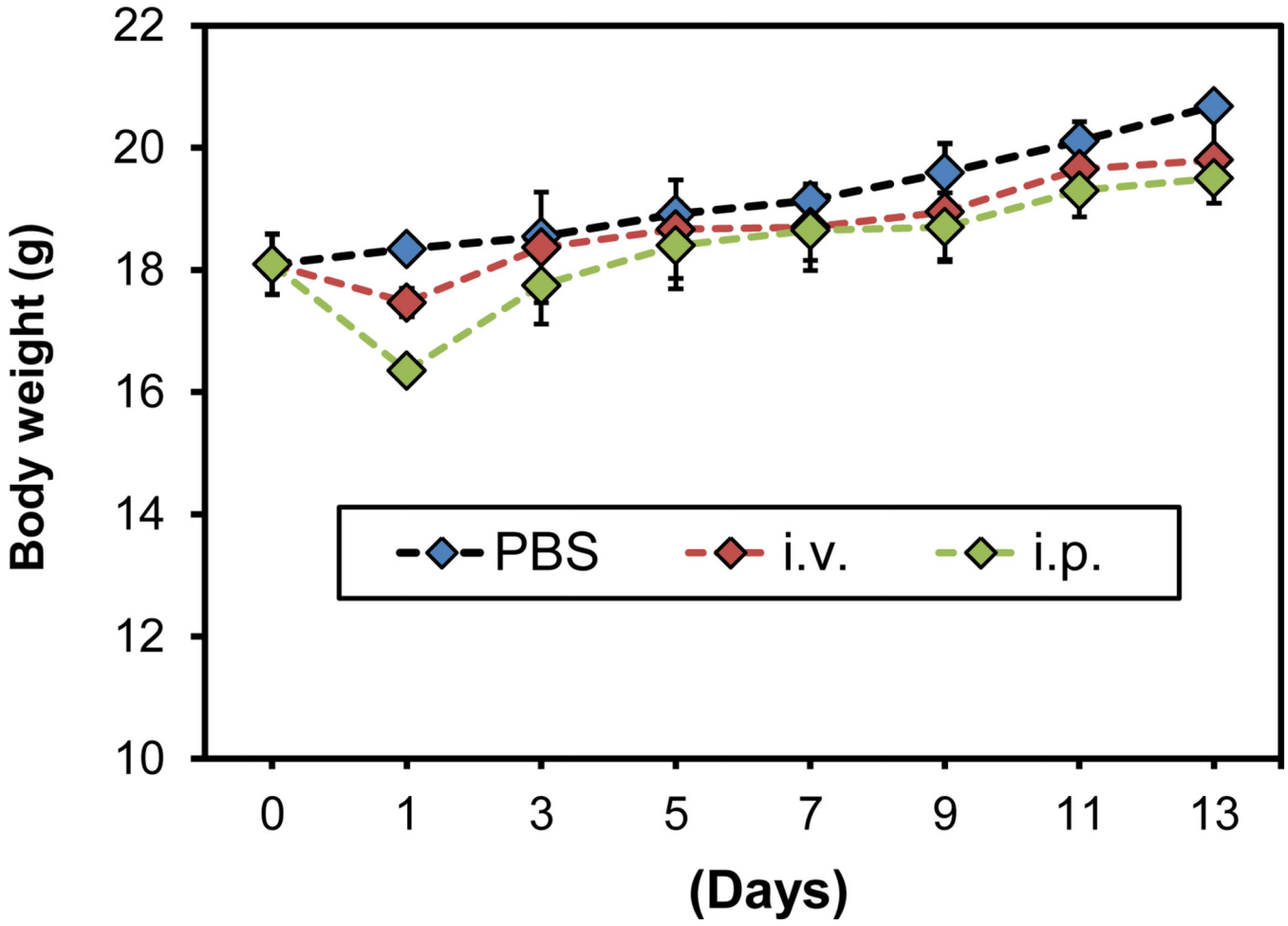

Fig. 2.

Body weight curves. Compared to the control group, the animals receiving either i.p. or i.v. injection of ferritins (50 mg/kg for i.p. injection and 15 mg/kg for i.v. injection) showed no significant weight loss except for a seemingly minor weight drop on day 1.

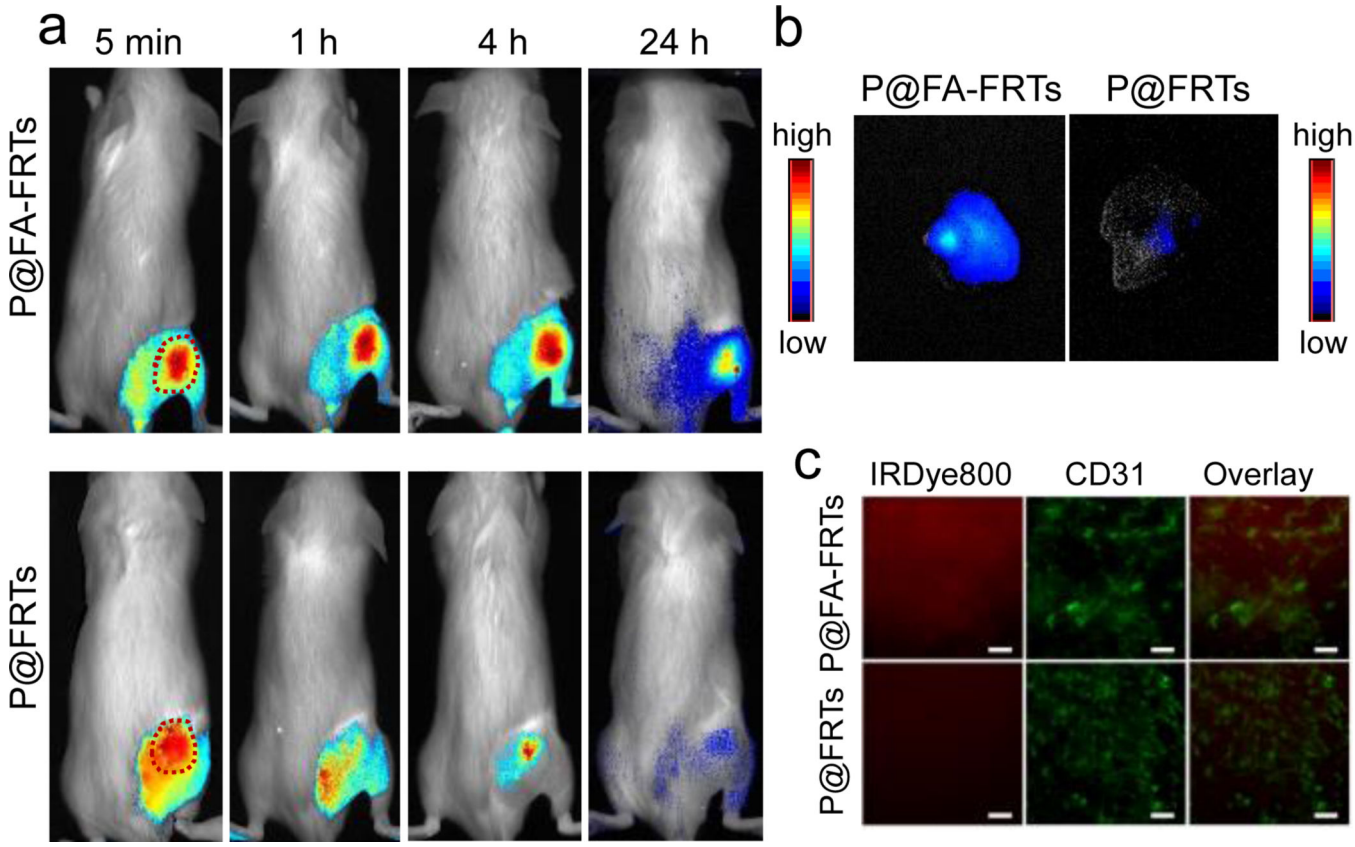

Fig. 3.

(a) *In vivo* tumour targeting, investigated with 4T1 tumour-bearing BALB/c mice. Compared with parental ferritins, P@FA-FRTs were more efficiently accumulated in tumours, especially for late time points. (b) *Ex vivo* imaging to compare tumour uptake between P@FA-FRTs and P@FRTs. (c) Immunofluorescence staining results. Consistent with the *in vivo* observation, stronger fluorescence signals were observed when the animals were injected with P@FA-FRTs. Red, IRDye800; green, phycoerythrin (anti-CD31). Scale bars: 100 μm.

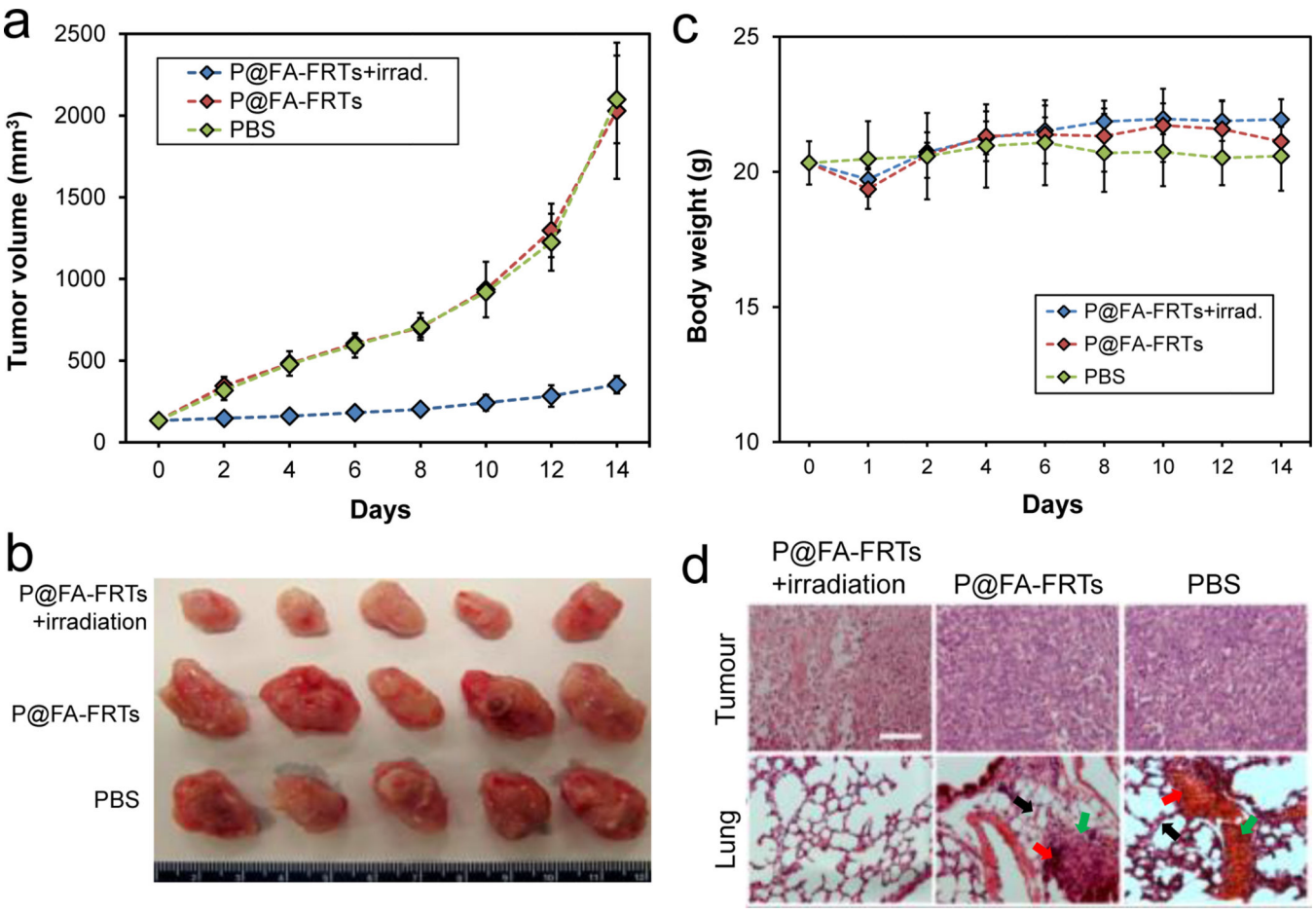

Fig. 4.

(a) Tumour growth curves. Significant tumour suppression was observed in animals treated with P@FA-FRT-mediated PDT. Compared to the control group, a tumour growth suppression rate of 82.65 ± 4.11 % was observed on day 14. (b) Photographs of dissected tumours from (a). (c) Body weight curves. No significant weight loss was observed for the treatment group. (d) H&E staining with tumour (upper) and lung (lower) samples. Significant necrosis was observed in tumours treated with P@FA-FRT-mediated PDT. In addition, while the control groups showed signs of metastasis in the lung (e.g. thickened alveolar membranes [black arrows], bleeding [red arrows], and inflammation sites [green arrows]), there was no sign of lung metastasis for PDT treated animals. Scale bar, 100 μm.